Anal. Chem. **2004,** *76,* 2273−2280

Potentiometric Titrations in a Poly(dimethylsiloxane)-Based Microfluidic Device

Rosaria Ferrigno,† Jessamine Ng Lee, Xingyu Jiang, and George M. Whitesides*

Department of Chemistry and Chemical Biology, Harvard University, 12 Oxford Street, Cambridge, Massachusetts 02138

This paper describes a microfluidic device, fabricated in poly(dimethylsiloxane), that is used for potentiometric titrations. This system generates step gradients of redox potentials in a series of microchannels. These potentials are probed by microelectrodes that are integrated into the chip; the measured potentials were used to produce a titration curve from which the end point of a reaction was measured.

The objective of this work was to design and characterize a microfluidic device that carries out potentiometric titrations and that uses serial dilution in preparing mixtures of analyte and reagent. Titration is one of the most widely used analytical techniques in quantitative analysis. Many types of titrations have been developed: for example, precipitation (Ag(I) with Cl^-, Br^-, I^-, SCN^-, or S^{2-}), complex formation (Ag(I) forming complexes with ligands such as CN^- or $S_2O_3^{2-}$), redox (Fe(II)/Fe(III) with Ce(III)/Ce(IV)), and acid−base.[1] The course of the titration can also be followed using many types of measurements: potentiometry, amperometry, spectrophotometry, turbidometry, fluorometry, and calorimetry.[2]

Two alternative methods have been developed in order to reduce the time required to carry out a titration: (i) automation of classical batch titration in a well-defined sample volume using an automated buret[3,4] and (ii) use of a continuous-flow system that generates a gradient of reactant.[5−8] In the latter method, flow rates that vary linearly with time generate a linear concentration gradient of the titrant.[9−11] The drawback of these systems is that they require a complex system of fluid handling and distribution in order to generate the titration curve.

Relatively complex systems have been designed to carry out titrations directly on-chip. For example, a system that requires the integration of static mixing chambers, electroosmotically driven pumps, separation membranes, platinum electrodes, and external electromagnetic valves was designed to run continuous volumetric titrations in microchannels.[12] In another device, generating the reagent electrochemically directly in a microchannel (for coulometric titration) eliminated the need for mixing.[12,13] These miniaturized systems require external power sources in order to generate the titrant electrochemically and to propel the fluid electroosmotically.

Reducing the overall size of the device, and measuring the required data in parallel, rather than serially, reduces the time required to complete a titration. This paper describes a microfluidic device that generates a titration curve using a simple procedure—by performing on-chip serial dilution of analyte and detecting the analyte in parallel using integrated electrodes. Here, the analyte and titrant solutions inject directly into the device and the solutions are allowed to flow by gravity. This device generates a range of concentrations of analyte in the form of step gradients using a system described previously.[14,15] It requires mixing of parallel streams in laminar flow; this mixing is efficient using a chaotic advective mixer (CAM).[16−18] A miniaturized immunoassay based on the same design has been demonstrated recently.[19] The device described here (i) requires only small volumes (<10 μL) of analyte and titrant, (ii) makes measurements of potential in parallel, and (iii) can perform the equivalent of a titration in continuous mode rather than in batch mode.

RESULTS AND DISCUSSION

Design of the Microfluidic Devices. We fabricated and used two different devices in this work. The first one (Figure 1) was very simple; it was used to characterize the efficiency of mixing

* To whom correspondence should be addressed. Telephone: (617) 495 9430. Fax: (617) 495 9852. E-mail: gwhitesides@gmwgroup.harvard.edu.

† Current address: Laboratoire d'Electronique, Nanotechnologie, Capteurs (LENAC), Bâtiment Léon Brillouin, Université Claude Bernard Lyon 1, 43 Boulevard du 11 Novembre 1918, 69622 Villeurbanne Cédex, France.

(1) Skoog, D. A.; West, D. M.; Holler, E. J. *Fundamentals of Analytical Chemistry*, 7th ed.; Saunders College Publishing: Philadelphia, 1996.
(2) Skoog, D. A.; West, D. M.; Holler, F. J. *Analytical Chemistry: an introduction*; Saunders College Publishing: Philadelphia, 1999.
(3) Cerda, V.; Ramis, G. *An introduction to laboratory automation*; John Wiley & Sons: New York, 1990.
(4) Valcarcel, M.; Luque de Castro, M. D. *Automatic methods of analysis*; Elsevier: Amsterdam, 1988.
(5) Nagy, G.; Feher, Z.; Toth, K.; Pungor, E. *Anal. Chim. Acta* **1977**, *91*, 87.
(6) Nagy, G.; Feher, Z.; Toth, K.; Pungor, E. *Anal. Chim. Acta* **1977**, *91*, 97.
(7) Pardue, H. L.; Fields, B. *Anal. Chim. Acta* **1981**, *124*, 39.
(8) Garcia, I. L.; Vinas, P.; Campillo, N.; Cordoba, M. H. *Anal. Chim. Acta* **1995**, *308*, 67.
(9) Alerm, L.; Bartroli, J. *Anal. Chem.* **1996**, *68*, 1394−1400.
(10) Ruzicka, J.; Hansen, E. H.; Mosbaeck, H. *Anal. Chim. Acta* **1977**, *92*, 235.
(11) Holman, D.; Christian, G.; Ruzicka, J. *Anal. Chem.* **1997**, *69*, 1763.
(12) Guenat, O. T.; Ghiglione, D.; Morf, W. E.; Rooij, N. F. d. *Sens. Actuators, B* **2001**, *72*, 273−282.
(13) Guenat, O. T.; Morf, W. E.; Schoot, B. H. v. d.; Rooij, N. F. d. *Anal. Chim. Acta* **1998**, *361*, 261−272.
(14) Dertinger, S. K. W.; Chiu, D. T.; Jeon, N. L.; Whitesides, G. M. *Anal. Chem.* **2001**, *79*, 1240.
(15) Jeon, N. L.; Dertinger, S. K. W.; Chiu, D. T.; Choi, I. S.; Stroock, A. D.; Whitesides, G. M. *Langmuir* **2000**, *16*, 8311.
(16) Stroock, A. D.; Dertinger, S. K. W.; Adjari, A.; Mezic, I.; Stone, H. A.; Whitesides, G. M. *Science* **2002**, *295*, 647.
(17) Stroock, A. D.; Whitesides, G. M. *Acc. Chem. Res.* **2003**, *36*, 597−604.
(18) Stroock, A. D.; Dertinger, S. K.; Whitesides, G. M.; Ajdari, A. *Anal. Chem.* **2002**, *74*, 5306−5312.
(19) Jiang, X.; Ng, J. M. K.; Stroock, A. D.; Dertinger, S. K. W.; Whitesides, G. M. *J. Am. Chem. Soc.* **2003**, *125*, 5294.

10.1021/ac035281i CCC: $27.50
Published on Web 03/19/2004

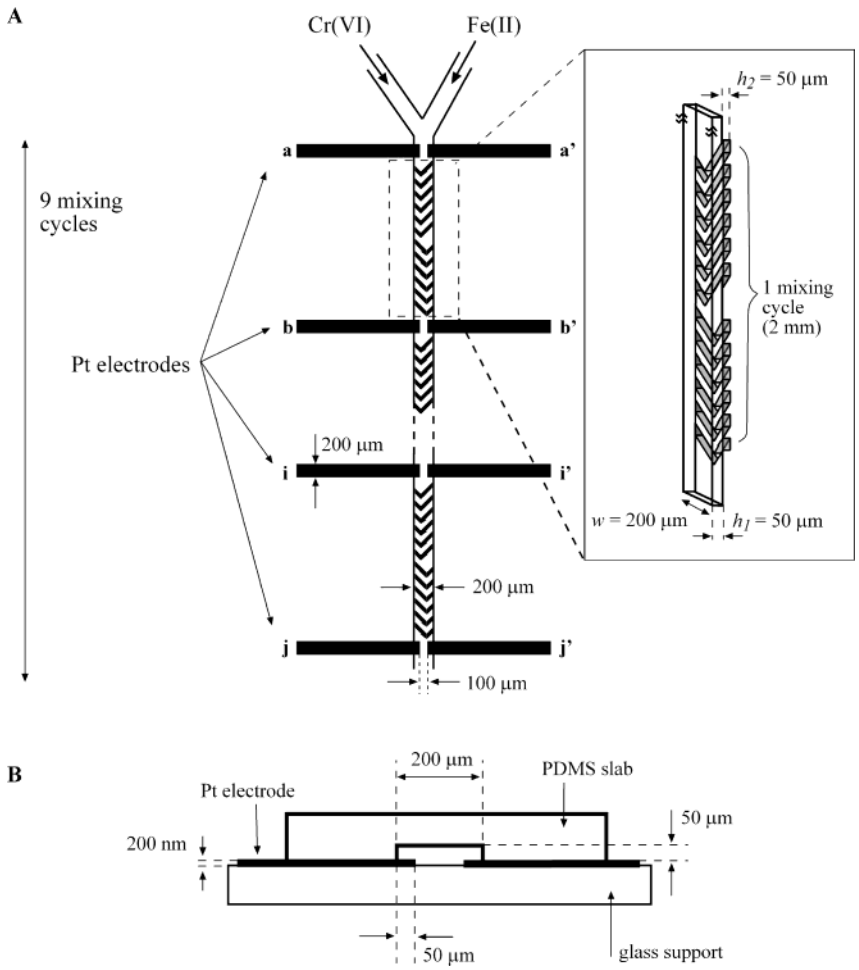

Figure 1. (A) Schematic representation of the device used to demonstrate that complete mixing is achieved in the potentiometric titration device. Ten pairs (e.g., (a, a′), (b, b′), ..., (j, j′)) of 200-nm-thick platinum electrodes were evaporated on a glass support. This glass support was used to close a channel embedded in PDMS. Each pair of dual-facing electrodes was located between two consecutive mixing cycles. Solutions of Fe(II) and of Cr(VI) were injected into the microchannel to probe the efficiency of mixing by potentiometry. One mixing cycle is composed of 12 herringbone structures; 9 cycles were located on the top wall of the microchannel (200 μm wide, 50 μm high with structures 50 μm high; see inset). Differences in potentials between pairs of dual-facing electrodes were measured and plotted as a function of the channel length. (B) Side view of the device used to characterize the efficiency of mixing. (Note: diagrams are not drawn to scale.)

using electrochemical tools. A potentiometric titration between an oxidant and a reductant requires an efficient mixing of the two solutions in order to ensure a fast reaction. In microfluidic channels, mixing of two solutions can be difficult due to the laminar behavior of the flow. Stroock[16] developed a CAM that used ribbed microstructures in the flow channel to solve this problem. We used the CAM in this work to ensure efficient mixing; we demonstrated the efficiency by performing electrochemical measurements. We used a simple microchannel with a Y-junction where we integrated ribbed microstructures, in the shape of herringbones, on the top wall of the channel (Figure 1). This microchannel system was fabricated using soft lithography.[20] A glass support bearing 10 pairs of platinum electrodes closed the microchannel. We assembled these two components of the microsystem with the help of an optical microscope to ensure good alignment of the microchannel with the electrodes. The electrodes were positioned in the microchannel between two consecutive herringbone cycles; the efficiency of mixing could thus be determined by measuring the potential between each pair of dual-facing electrodes after each mixing cycle.

The second device fabricated in this work incorporates a serial dilutor[19] that mixes and dilutes a sample solution with a titrant solution (Figure 2). The dilution process produces a series of solutions containing exponentially decreasing redox potentials; these potentials are used to generate a titration curve. A typical system comprised a network of 11 channels (50 μm deep and 100 μm wide, Figure 3A). Two distinct inlet reservoirs supplied (i) the sample that was analyzed and (ii) the titrant solution. At the junction (200 μm wide) between the channel supplying the sample solution and the channel supplying the titrant solution (both channels 100 μm wide), herringbone microstructures (nine cycles) placed on the top wall of the junction ensured efficient mixing and complete reaction between the sample and the titrant solutions.[16,21] We designed the serial dilutor to have a dilution factor of ~2; that is, at each junction, the solution injected into inlet 1 splits into two halves. One stream flows to the outlet (waste) without further dilution; the other mixes 1:1 with the solution injected into inlet 2 (and thus the concentration of the resulting

(20) Duffy, D. C.; McDonald, J. C.; Schueller, O. J. A.; Whitesides, G. M. *Anal. Chem.* **1998**, *70*, 4974−4984.

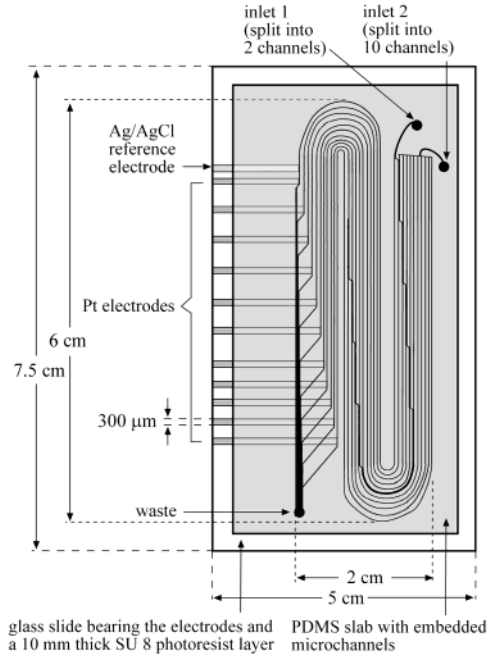

Figure 2. Top view schematic representation of the complete microfluidic device. The device consists of a channel network embedded in a PDMS slab, sealed against a glass slide bearing the platinum electrodes at the end of the network. Each electrode was in contact with one channel; the reference Ag/AgCl electrode was located in the first channel. (Note: diagrams are not drawn to scale.)

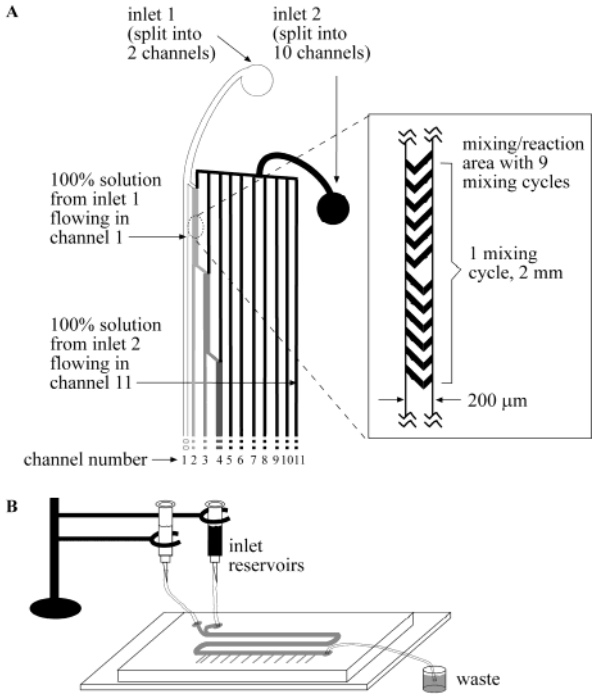

Figure 3. Schematic diagram illustrating the dilution of the solutions allowed to flow into the inlets of the device presented in Figure 2. (A) The solution injected into inlet 1 splits into two channels. The first channel contains 100% solution from inlet 1 (shown here in white); the second channel is serially diluted and reacts with the solution injected from inlet 2 (shown here in black). At the mixing areas (three are shown), nine cycles of herringbone structures were integrated into the microchannels to obtain efficient mixing (inset). Channels in the mixing areas were twice as wide (200 μm) as channels in the nonmixing areas. (B) Side view diagram depicting the injection of solutions into inlets 1 and 2 by gravity. Solutions were contained in inlet reservoirs (5-mL syringes) that were open to air; they were connected to the microchannels via polyethylene tubing. The flow rates of each of the solutions were controlled by the height of the syringes. The outlet of the channel system connected to a waste reservoir via polyethylene tubing. (Note: diagrams are not drawn to scale.)

solution decreases, Figure 3A). A more thorough description of the dilutor can be found in refs 14 and15.

The electrochemical measurements took place at the end of the channel system, just before all of the microchannels reconnected to produce a waste stream. At these detection points (Figure 4), small apertures (100 μm × 100 μm) in a thin layer of photoresist (10 μm) allowed contact between an electrode and the solution flowing in the channel above it. In all other areas where the electrodes crossed the channels, the layer of photoresist insulated the solution from the electrodes. An optical microscope aided the alignment between the PDMS slab and the electrodes.

During operation, we injected two solutions into the device: one was a strong oxidant, $Cr_2O_7^{2-}$ (Cr(VI)), used as the titrant, and the other was a reducing species, $Fe(CN)_6^{4-}$ (Fe(II)), used as the sample. To each of the solutions we added ~ 0.1 M KCl and ~ 10^{-3} M HCl (until each solution reached pH ≅3) to provide the acidic condition necessary for the titrations and the electrolyte composition required by the Ag/AgCl reference electrode. We placed the reservoirs containing the titrant and sample solutions ~30 cm above the device (Figure 3B). We allowed these solutions to flow into inlets 1 and 2 by gravity. The flow rate, measured at the end of the channel system, was ~1 μL/s. The level of fluid in each of the reservoirs was nearly constant during the duration of the experiments (few minutes), since the volume of solution in the reservoir was large (~3 mL) compared to the volume of solution in the microchannels (~6 μL). The *relative* flow rates of the sample and the titrant solutions were calibrated before use by adjusting the heights of the reservoirs. Differences in pressure and flow rate in the two channels change the dilution factor of the device and, therefore, may contribute to inaccuracies in the measurements. Although we allowed the titrant and sample solutions to flow by gravity, it is also possible to use other methods to pump the fluids, such as by using syringe or electrical pumps.

Once the microchannels had filled completely (total internal volume ~6 μL), the potentials were measured manually at the electrodes using a voltmeter. Simultaneous measurements in each channel may take only a few seconds by combining an electronic readout system (e.g., LabVIEW) to this microdevice. At the end of the channel network, the fluid in each channel combined into a waste stream. The output stream (here, "waste") has the characteristic of a controlled lateral gradient in redox potential; this gradient may be useful for other applications.[14,22]

Characterization of the Microfluidic Devices. We first characterized the efficiency of mixing electrochemically using the

(21) We balanced the inherent pressure drop induced by these herringbone structures by placing on the top wall of the remaining channels (channels where mixing was not required) structures that occupied the same volume as the herringbone structures but that did not promote efficient mixing. These structures were rectangular and positioned 45° to the direction of the flow (see ref 18).

(22) Dertinger, S. K. W.; Jiang, X. Y.; Li, Z. Y.; Murthy, V. N.; G. M., W. *Proc. Natl. Acad. Sci. U.S.A.* **2002**, *99* (20), 12542−12547.

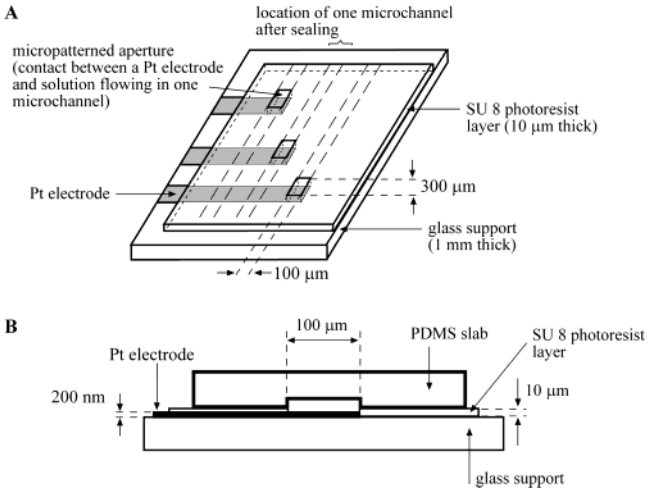

Figure 4. (A) Top diagonal view of a thin layer (10 μm) of SU 8 spun on a glass slide after the evaporation of the microelectrodes on the slide (microfluidic channels are not shown for clarity). This layer was patterned such that only one microelectrode was in contact with solution flowing in one microchannel through an aperture in the layer. (B) Side view of a channel of the device where a Pt microelectrode is in contact with the solution flowing in the channel. (Note: diagrams are not drawn to scale.)

system described in Figure 1. We compared mixing at different points along a single channel with nine sections of CAM to mixing along a channel without the herringbone structures. We integrated platinum electrodes on each side of the channel in both microchannels (Figure 1); these electrodes faced each other and were 100 μm apart across the width of the channel. Each pair of electrodes separated the next pair by 2 mm along the length of the channel. Figure 5 describes the potential measured between a series of these dual-facing platinum electrodes when solutions of Fe(II) and Cr(VI) were flowing in a single channel. Without the mixing structures, flow in the channel was laminar and mixing of the reagents was due only to the diffusion of the ions across the channel: the potential thus varied only slightly along the channel, as the rate of mixing of the reagents was slow. Without a mixing section, complete mixing was not achieved by the end of the channel; the difference in potential between the last pair of facing Pt electrodes reached a value of ~250 mV. Incorporating the mixing sections caused the potential to decrease after each CAM section and enabled the potential to reach ~0 mV at the end of the microchannel; this value indicates that complete mixing has occurred. From Figure 5, we infer that mixing is approximately complete after five sections of the CAM at a flow rate of ~1 μL s^{-1}.

We characterized the microfluidic titration device represented in Figure 2 by allowing fluorescein to pass through inlet 1 and water to pass through inlet 2 and measuring the changes in fluorescence intensity in each channel (using a fluorescence microscope) after each successive dilution. We designed this device to obtain an exponential dilution pattern at the outlet with a theoretical dilution factor of 2.[19] In our experiments, we measured a dilution factor of 2.2, averaged over all of the junctions of the device and over three different experiments. The relationship between c and n is exponential (eq 1) where c_n is the concentration of the analyte in channel n (where n ranges from 1 to 11 in this work) and c is the initial concentration:

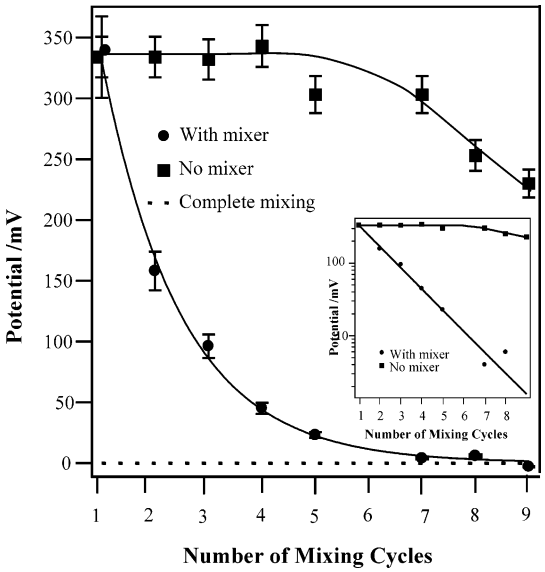

Figure 5. Potential measured between dual-facing platinum electrodes (e.g., (a, a′), (b, b′), ..., (j, j′)) as a function of their location along the microchannel represented in Figure 1. The solutions injected into the inlets were 5 mM $Cr_2O_7^{2-}$ (Cr(VI)) and 0.1 M $Fe(CN)_6^{4-}$ (Fe(II)); both solutions contained 0.1 M KCl and 10^{-3} M HCl and had a pH ≅3. Location of the dual-facing electrodes is reported here as the number of mixing cycles away from the inlets, where each cycle measured 2 mm. The lines on the plot were drawn to guide the reader. The error bars represent the range of potentials measured for three different experiments. The inset shows the potentials represented in a logarithmic plot.

$$c_n = (1/2.2^{n-1})c \qquad (1)$$

Channel $n = 1$ corresponds to the channel that contains the solution injected into inlet 1 (0% dilution). Channel $n = 11$ corresponds to the channel that contains 100% of the solution injected into inlet 2; i.e., this solution flows to the end of the device without being mixed with any solution from inlet 1.

In the case of potentiometric measurements, if a redox-active species (a reductant R, for example) is injected into inlet 1, the potentials measured in each channel follow the Nernst equation and are therefore proportional to the logarithm of the concentration in each channel, i.e., $E \propto \ln(c)$, if the concentration of the oxidant is kept constant. The relationship between E and n is thus linear for the case of these channels for a constant concentration of oxidant (eq 2).

$$E_n = E^\circ + \frac{RT}{\alpha F}\ln(c_{Ox}) - \frac{RT}{\alpha F}\ln(c) + \frac{RT}{\alpha F}\ln(2.2)^{(n-1)} \qquad (2)$$

Here c_{Ox} is the constant concentration of the oxidant, α the number of electrons exchanged between the reductant and the oxidant, E° the formal redox potential of the oxidoreductant couple, R the gas constant, T the temperature, and F the Faraday constant. Thus, an exponential concentration gradient of a redox species results in a linear gradient of the electrochemical potential.

Generation of a Potentiometric Titration Curve. We investigated the redox systems Fe(II)/Fe(III) and Cr(III)/Cr(VI) in the microfluidic device shown in Figure 2. The redox reaction between Cr(VI) ($Cr_2O_7^{2-}$, considered here as the titrant) and

Fe(II) ($Fe(CN)_6^{4-}$, considered as the sample) is summarized by eq 3. The network offered two injection schemes: (i) the case

$$Cr_2O_7^{2-} + 6Fe(CN)_6^{4-} + 14H^+ \rightarrow 2Cr^{3+} + 6Fe(CN)_6^{3-} + 7H_2O \quad (3)$$

where we injected the sample into inlet 1 and the titrant into inlet 2 and (ii) the reverse case, where we injected the titrant into inlet 1 and the sample into inlet 2. We infer that the choice of the injection scheme has an influence on the detection limit of the device.

We first investigated the case where the sample, a solution of Fe(II) (100 mM), was injected into inlet 1 and the titrant solution of Cr(VI) was injected into inlet 2. To have an optimal determination of the sample concentration, the titration end point (i.e., the point in the titration where 99% of the sample has reacted with the titrant) has to be located in one of the middle channels of our device (i.e., $3 < n < 8$). The location of the titration end point depends on the relative concentrations of the sample and the titrant. We investigated three different concentrations of Cr(VI)—0.05, 0.5, and 50 mM—in order to demonstrate the influence of this parameter on the location of the titration end point in the channel. Figure 6A shows the potentials measured in each channel relative to a common Ag/AgCl reference electrode; the data are plotted against the channel number, *n*.

Since the representation *E* versus *n* (Figure 6A) does not allow a straightforward recognition of the titration end point, and because a sigmoidal shape is more convenient for determining this point, we applied the function defined by eq 4 to our experimentally measured potentials.[23] Here, $E_{min(Fe)}$ is the potential measured when the solution of the sample contains only Fe and no Cr (that is, in channel 1), $E_{max(Cr)}$ is the potential measured when the solution of the titrant contains only Cr and no Fe (that is, in channel 11) and *n* ranges from values of 2 to 10.

$$\phi_n = \ln\left[\left(\frac{E_{min(Fe)} - E_{max(Cr)}}{E_n - E_{max(Cr)}}\right) - 1\right] = \ln\left[\left(\frac{E_1 - E_{11}}{E_n - E_{11}}\right) - 1\right] \quad (4)$$

This mathematical expression is derived from the sigmoid function, eq 5, which gives a sigmoidal relationship between any parameters *y* and *x*; A_1 and A_2 are two constants defining the minimum and the maximum values that can be reached by *y*, x_o is the abscissa corresponding to the midpoint between A_1 and A_2, and d*x* is a normalizing factor.

$$y = \frac{A_1 - A_2}{1 + e^{(x - x_o)/dx}} + A_2 \quad (5)$$

Equation 5 can be rewritten as eq 6 when applied to our problem, where *n* ranges from values of 2 to 10. Equation 4 allows the

$$E_n = \frac{E_{min} - E_{max}}{1 + e^{\phi}} + E_{max} = \frac{E_1 - E_{11}}{1 + e^{\phi_n}} + E_{11} \quad (6)$$

redistribution of the experimental points between a maximum and a minimum value. In eq 4, when the function ϕ equals 0, the potential corresponds to the inflection point of the sigmoid, i.e., the end point of the titration.

Figure 6B shows the sigmoidal representations of the experimental points presented in Figure 6A that were obtained using

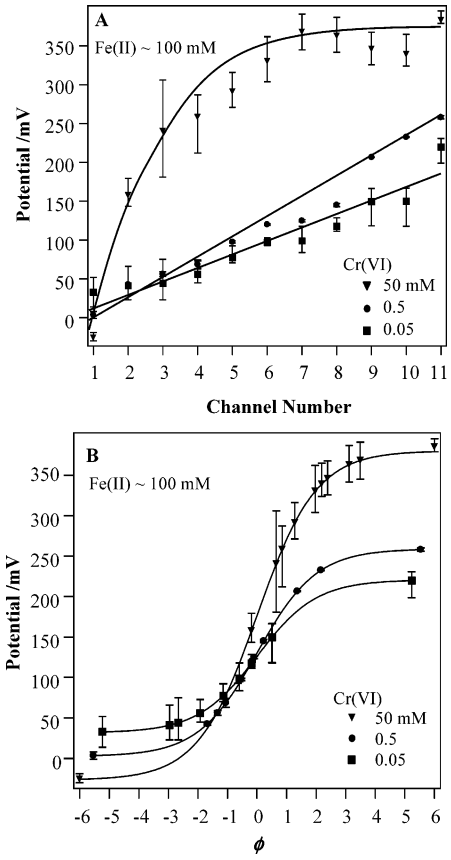

Figure 6. Potentiometric curves obtained for the titration of Fe(II) at a concentration of 100 mM (inlet 1) with Cr(VI) at different concentrations: 0.05, 0.5, and 50 mM (inlet 2). The supporting electrolyte, added to each of the solutions, was 0.1 M KCl and 10^{-3} M HCl. Each of the solutions had a pH ≅3. (A) Potential as a function of the channel number. (B) Potential as a function of the function ϕ (eq 4). The lines on the plot were drawn to guide the reader. The error bars represent the range of potentials measured for three different experiments. We attribute this error mainly to the fluctuations of the potential of the Ag/AgCl reference electrodes over time; these fluctuations are due to the reference electrode being directly in contact with the solutions injected into the microdevice.

(23) We tried plotting the potential as a function of the ratio of the volume of Fe(II) to Cr(IV), but this plot does not give a sigmoidal curve. A sigmoidal curve was not obtained, due to the superimposition of two phenomena that cause the depletion of the sample in this titration: (i) dilution of the titrant and (ii) reaction between the titrant and the sample at each junction (i.e., during each dilution). The case presented in this paper is more complex than that of a classical batch titration experiment. In the case of a classical batch titration experiment, the potential *can* be plotted against the ratio of the volume of Fe(II) to Cr(IV) to give a sigmoidal curve, since this ratio is directly proportional to the volume of titrant, and the depletion of the sample in the beaker depends only on the reaction with the titrant. Our case, however, is more complicated, because the concentration of titrant is different at each junction (due to dilution and reaction of the titrant). The volume of titrant (or a ratio using this volume), thus cannot be used to follow the progress of the reaction. We therefore plotted the potential against ϕ, a function that gives a sigmoidal relationship between the points (here, the potential vs channel number) and "adjusts" the points in order to fit them in the form of a curve. The end point can then be determined graphically by finding the inflexion point of the sigmoid, where $\phi = 0$.

Table 1. Comparison between the Titration End Point Determined by Experiments (Exper End Point) and by Calculations (Theor End Point)

[Fe(II)] (mM)	[Cr(VI)] (mM)	end point: theor (channel no.)	end point: exper[a] (channel no.)
A. Solution of Fe(II) Injected into Inlet 1 and Cr(VI) into Inlet 2 (Figure 6)			
100	0.05	10	9
100	0.5	7	7
100	50	2	3
B. Solution of Cr(VI) Injected into Inlet 1 and Fe(II) into Inlet 2 (Figure 7)			
10	50	6	5
10	5	4	3
1	5	6	5

[a] Denotes an average of three experimental measurements (±1 channel).

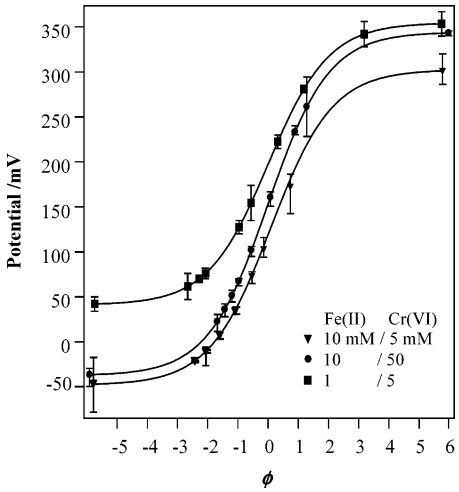

Figure 7. Potentiometric curves obtained for the titration of Fe(II) at concentrations of 10 and 1 mM (inlet 2) with Cr(VI) at different concentrations 5 and 50 mM (inlet 1). The supporting electrolyte, added to each of the solutions, was 0.1 M KCl and 10^{-3} M HCl. Each of the solutions had a pH ≅3. The lines on the plot were drawn to guide the reader. The error bars represent the range of potentials measured for three different experiments. We attribute this error mainly to the fluctuations of the potential of the Ag/AgCl reference electrodes over time; these fluctuations are due to the reference electrode being directly in contact with the solutions injected into the microdevice.

this transformation. For the case of a 0.5 mM solution of Cr(VI) and a 100 mM solution of Fe(II), the titration end point determined by our experimental measurements (which we call the "experimental end point") corresponded to channel 7, in good agreement with the titration end point determined by calculations (which we call the "theoretical end point"). Table 1A summarizes the influence of the relative concentrations between the titrant and the sample on the titration end point. Table 1A also shows comparisons between experimental and theoretical end points for three different Cr(VI) concentration values. We observe that the channel number where the titration end point was determined experimentally shifted in agreement with the calculations.

This injection scheme could only detect a high concentration of sample (Fe(II), ∼100 mM) and would require titrating against a very low concentration of Cr(VI) (<0.05 mM) to reach a lower detection limit of Fe(II). To decrease this detection limit, we investigated the second injection scheme available with our device, i.e., by injecting the sample Fe(II) into inlet 2 and the titrant Cr(VI) into inlet 1. Figure 7 shows the curves obtained for various concentrations of Fe(II) and Cr(VI), and Table 1B compares these values with ones predicted by calculations. The advantage of using this configuration is that we were able to reach a lower detection limit of ∼1 mM for Fe(II), a value usually reached by conventional potentiometric titrations.[13] We also evaluated this device for the titration of I^- with $S_2O_8^{2-}$ (data not shown) and found a similar agreement between the experimental and theoretical titration end points.

The present accuracy of this device is ±1 channel. The shift of the titration end point of one channel corresponds to a variation of the sample concentration by a factor of ∼3−5-fold (since a 10-fold change in the concentration of the starting sample resulted in a shift of end point between 2 and 3 channels, Table 1). This accuracy is low compared to a batch experiment (∼2%).

CONCLUSIONS

This paper demonstrates the design and fabrication of a microfluidic device made in PDMS for performing on-chip potentiometric titrations. This device incorporates mixing elements, a serial dilution system, and microelectrodes; it is easy to fabricate, simple to operate, and does not require an external power source to pump the reagents. The system works in a continuous mode by using a gradient generator system to allow several chemical reactions between sample and reagent to take place in parallel. The integrated electrodes enable us to follow each of these reactions, and thus, we can generate a full titration curve in one step. Acquiring the measurements in parallel greatly decreases the time required to determine the titration end point compared to a titration system that operates serially. This device can carry out potentiometric titrations on-chip with much smaller quantities of titrant and sample (<10 μL) than a buret, which is used for classical batch titrations (>1 mL).

We showed that this device determined the titration end point of an ∼1 mM sample; this detection limit is comparable to that obtained by conventional potentiometric titration techniques. The accuracy of this device, however, was low. We did not show optimizations of this device in terms of sensitivity and accuracy, but these optimizations can be achieved by increasing the number of channels, decreasing the dilution factor (and thus, the dynamic range) used in the device by changing the relative pressures of the sample and titrant, and by changing the type of electrodes.

To determine unknown sample concentrations, this device will require preliminary calibrations, which we did not perform in this work.[24] In addition, the electrodes used in this work were not selective to one redox couple and were therefore not suited for the quantification of mixtures. The quantification of real sample mixtures may require the integration of multiple selective electrodes, such as copper, lead, or silver electrodes, in each microchannel. The integration of these electrodes is more challenging from a technological standpoint than what we have presented here, because selective electrodes require a more complicated design due to the presence of selective layers and internal references.[25]

The use of this system can extend to other applications by using other electrochemical methods, such as amperometry, to detect the end point. Amperometry can be a sensitive and selective technique that would allow the detection of analytes that cannot be detected using potentiometry (e.g., glucose).

EXPERIMENTAL SECTION

Materials. Sylgard 184 Silicone, a two-part poly(dimethylsiloxane) (PDMS) elastomer, was purchased from Essex Brownell (Edison, NJ). For all devices, we used a 10:1 (by weight) mixture of PDMS base/curing agent that was degassed under vacuum and cured at 70 °C for ∼24 h. The reagents $Fe(CN)_6^{4-}$ (Fe(II)), $Cr_2O_7^{2-}$ (Cr(VI)), I^-, $S_2O_8^{2-}$, KCl, and HCl were obtained from Sigma-Aldrich Co. (St. Louis, MO) and used as received; solutions of these reagents were made in 18 MΩ water. All other chemicals were purchased from Sigma-Aldrich Co. and used as received unless indicated otherwise.

Fabrication of the Microfluidic Devices. (See Supporting Information for more details on the fabrication of this device.) We fabricated channels that were 50 μm high and had various structures (e.g., herringbone) on the top walls of the channels that were also 50 μm high. The channels were fabricated in PDMS by replicating a master obtained by conventional photolithography.[20,26] The SU-8 channel structure on the master was prepared on a silicon wafer by a two-step photolithographic process described elsewhere.[16] We aligned the channels embedded in PDMS to a glass slide bearing the platinum electrodes under an optical microscope; we sealed the device by using clamps that applied a small pressure to the device. The PDMS slab and the glass slide therefore sealed reversibly; this reversible seal allowed us to reuse the glass slide bearing the electrodes several (∼5) times.

Fabrication of the Electrode System. We used plain microscope slides (75 × 50 × 1 mm, borosilicate glass, Corning, NY) as supports for the electrodes and to close the channels embedded in PDMS. To fabricate the electrodes, the glass slides were first cleaned (using water and ethanol) and then treated with hexamethyldisilazane (Microelectronics Materials Corp.) to promote the adhesion of the Shipley 1813 photoresist (Microchem Corp.). We spin-coated the photoresist at 500 rpm for 5 s and at 4500 rpm for an additional 30 s to give a thickness of ∼1.2 μm. The slides were then placed directly on a digital hot plate set at 105 °C, baked for 3 min, and promptly removed. A CAD program was used to design the shape of the electrodes; this design was printed onto a transparency film (PageWorks, Cambridge MA), which served as a photomask for photolithography.[27] The photomasks were placed on top of the resists, and the resists were exposed to UV light for 6 s at 50 mJ s^{-1}. We then immersed them in fresh 351 developer (Microchem Corp., composition 80% NaOH and 20% H_2O) with agitation from a Branson 251 sonifier (VWR Corp.). Within 1 min, the exposed regions began to exude a red color, indicating that development of the photoresist had begun. We continued the agitation until formation of the red color ceased and the resulting pattern attained a uniform appearance (∼30 s). After rinsing the slides thoroughly with 18 MΩ water, we dried them under a stream of N_2. We evaporated sequentially 7.5 nm of titanium (to promote adhesion) and 200 nm of Pt onto the patterned slides using an electron beam evaporator. We removed the remaining photoresist by immersing the slides in an acetone (or ethanol) bath and then sonicating them. Peeling off the photoresist revealed the metallic patterns formed on the slides that were to be used as electrodes.

Alignment of the electrodes and microfluidic channels is shown in Figure 4A. Since all of the electrodes (except for the first) cross under several channels of the system, the electrodes needed insulation from all of the channels except one, where detection takes place. Here, we let each electrode detect the solution in the right-most channel crossing over the electrode. In each of these positions, a small aperture (100 μm × 100 μm) in a thin layer of photoresist allowed contact between the electrode and the solution flowing in the channel above it. To make this insulating layer, a thin layer (∼10 μm) of SU 8-2005 photoresist (Microchem Corp.) was spun (5 s at 500 rpm and 15 s at 900 rpm) on the glass bearing the electrodes. We aligned a photomask having the pattern of the apertures on top of the electrodes, and exposed this system to UV light. We developed the resist in a propylene glycol methyl ether acetate bath for 2 min, leaving the apertures (100 × 100 × 10 μm, *lwh*) in the resist.

One of the platinum microelectrodes was converted to a reference Ag/AgCl electrode by applying a potential difference of 800 mV between the Pt integrated microelectrode and an external Pt macroelectrode. We immersed the electrodes in a solution of commercial silver bath (Techni-Silver EHS-3, Technic Inc.), and we polarized the Pt microelectrode as a cathode in order to electroplate Ag on the Pt. Then, after immersing the electrodes into a saturated KCl solution, we applied a potential difference of 800 mV for ∼15 s to the electrodes (the newly formed Ag/Pt electrode polarized anodically), to form an AgCl layer (∼100 nm in thickness).

Measurements. To perform the experiments, solutions of titrant and sample were placed in 5-mL syringes (Becton, Dickinson and Co.) without the plunger; these syringes were used as reservoirs. We attached these syringes to polyethylene tubing (Intramedic, PE 20) that connected to the inlets of the device. The solutions were allowed to flow by gravity. We clamped the reservoirs to a stand; the flow rate of each solution was adjusted

(24) The device can be used to monitor unknown concentrations of sample by first generating a calibration curve. This plot would be made by performing the same types of experiments as demonstrated for device 2 in this paper, using a series of solutions of sample that range in concentration (these concentrations are known). For example, if the goal was to determine an unknown concentration of $Fe(CN)_6^{4-}$, a series of solutions of known concentration of $Fe(CN)_6^{4-}$ (e.g., 0.1, 0.5, and 1 mM $Fe(CN)_6^{4-}$, etc.) would have to be made. Device 2 would be used to titrate each of these solutions of $Fe(CN)_6^{4-}$ against the same concentration of titrant, $Cr_2O_7^{2-}$. This procedure would allow the determination of the end point (measured by the channel number, where $\phi = 0$) for each of these experiments. Then, a calibration curve can be generated with these data by plotting the concentration of $Fe(CN)_6^{4-}$ on the *y*-axis, against the channel number where the end point occurred on the *x*-axis. Determining the (unknown) concentration of a sample of $Fe(CN)_6^{4-}$ would require titrating the unknown solution against $Cr_2O_7^{2-}$ (the same concentration of $Cr_2O_7^{2-}$ used to generate the calibration curve) and determining the channel where the end point occurred. The concentration of the unknown sample can be determined by correlating the channel number to the corresponding concentration of $Fe(CN)_6^{4-}$ using the calibration curve.

(25) Tantra, R.; Manz, A. *Anal. Chem.* **2000**, *72*, 2875.

(26) McDonald, J. C.; Whitesides, G. M. *Acc. Chem. Res.* **2002**, *35*, 491−499.

(27) Ng, J. M. K.; Gitlin, I.; Stroock, A. D.; Whitesides, G. M. *Electrophoresis* **2002**, *23*, 3461−3473.

by changing the height of each reservoir. The relative flow rates of the solutions in inlets 1 and 2 were calibrated to obtain 1:1 splitting at each junction by viewing the splitting under an optical microscope. Flow rates were measured at the outlet (waste) by weighing the amount of solution recovered at the end of the device during a fixed period of time.

We measured the difference in potential between a Pt electrode located in one of the channels and the Ag/AgCl reference electrode using a Fluke 75 Multimeter. We connected one Pt electrode to the voltmeter, took the measurement, disconnected the electrode, and then connected the adjacent one. The measurements can be detected simultaneously by connecting the electrodes of a device to a connector block (e.g., TBX-68 I/O, National Instruments), which sends electronic signals to a data acquisition card (e.g., PCI card) that connects to a computer. The signals can be read by a software program such as LabVIEW (National Instruments).

ACKNOWLEDGMENT

This work was funded by the NIH (GM65364) and the DARPA/NSF (ECS-0004030). R.F. is grateful to the Swiss National Science Foundation for a postdoctoral fellowship. J.N.L. thanks the National Science and Engineering Research Council of Canada (NSERC) for a postgraduate scholarship.

SUPPORTING INFORMATION AVAILABLE

Additional information as noted in text. This material is available free of charge via the Internet at http://pubs.acs.org.

Received for review October 30, 2003. Accepted February 11, 2004.

AC035281I